

Aerosol Sulfate Loading and Shortwave Direct Radiative Forcing over the North Atlantic Ocean

S. Nemesure, C. M. Benkovitz and S. E. Schwartz
 Environmental Chemistry Division
 Brookhaven National Laboratory
 Upton, New York

Introduction

Shortwave radiative forcing of climate by anthropogenic sulfate aerosols is estimated to be equal in magnitude but opposite in sign to that of greenhouse warming, with a global annual average value of approximately -1 W m^{-2} uncertain to at least a factor of two. Contribution estimates to this forcing by the direct effect are -0.4 W m^{-2} . It is therefore necessary to accurately and efficiently represent this forcing in climate models, specifically including spatial and temporal variability.

Here we explore a method to expedite the process for determining this forcing. The method utilizes an approach where the forcing is computed precisely at several discrete radii (r) and then integrated over an arbitrary aerosol size distribution. Additionally, the forcing is calculated at several values of relative humidity (RH), solar zenith angle (SZA), and aerosol optical thickness (τ). The parameters can be interpolated to provide the forcing at specific intermediate values. Alternatively, an empirical relationship between the forcing and the above mentioned variables can be utilized to further reduce computation time. At present, the calculations are restricted to ammonium sulfate particles over an ocean surface. The advantage of the ocean surface is the constant and low albedo compared to the highly variable albedo of land surfaces. Ultimately, the sensitivity of forcing to surface albedo and composition will be included.

The strategy for this approach is to calculate the aerosol forcing for several "narrow" distributions centered about a discrete number of radii. The forcing at each of these radii can readily be integrated for an arbitrary size distribution as a weighting factor to produce the forcing for that arbitrarily selected aerosol size distribution. The optical properties and aerosol phase functions, $P_{\lambda}(\Theta)$ for ammonium sulfate aerosol were calculated assuming a gamma particle size distribution ("effective variance" equal to 0.01) wide enough to remove any resonances in the particle size range considered, yet narrow enough that the Mie scattering properties were calculated essentially for monodisperse aerosols. A doubling and adding multiple scattering model (Hansen and Travis

1974) was then used to compute the forcing at each of these discrete radii. The forcing for the arbitrary aerosol number distribution n_i was then expressed as

$$F = \frac{\sum_i f_i n_i k_i \delta r_i}{\sum_i n_i k_i \delta r_i} \quad (1)$$

where f_i is the forcing per optical thickness calculated for a narrow size distribution centered about the i 'th radius, k_i is the extinction coefficient, and r_i represents the incremental width of the i 'th radius interval. k is necessary in Equation (1) to convert the forcing per optical thickness, f_i , to a forcing normalized to particle loading since the size distribution, n_i , is a number distribution. Figure 1 shows the spectrally averaged forcing (see Coakley et al. 1983; Nemesure et al. 1995 for an explanation of the spectral average calculation) as a function of $\mu_0 = \cos(\text{SZA})$ calculated for a marine aerosol size distribution (Hoppel et al.

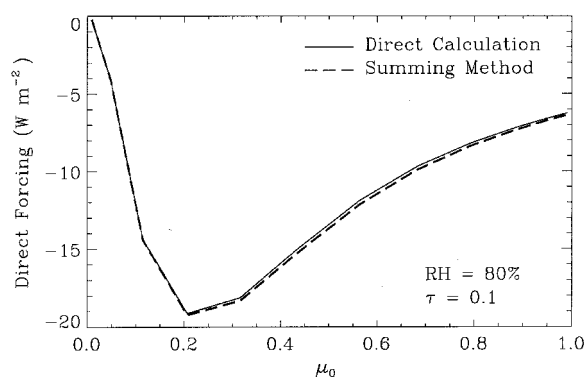


Figure 1. Dependence of direct forcing, ΔF on $\mu_0 = \cos(\text{SZA})$ for a relative humidity, $\text{RH} = 80\%$ and optical thickness, $\tau = 0.1$ calculated by the summing method (dashed line) and the direct method (solid line) using the marine aerosol size distribution (Hoppel et al. 1990).

1990) using the above method. In addition, a “brute force” calculation, where the optical properties and phase function for the marine distribution were used in the implementation of the multiple scattering model is also shown for comparison. The accuracy of the approximate method is quite good, with our summing method overestimating the “brute force” forcing by less than one percent. At other values for RH and τ , the accuracy may be slightly better or worse depending on the linearity between these variables and the forcing. The accuracy of the forcing can be somewhat improved if a more appropriate relationship between the aerosol forcing and these variables can be defined. For example, a simple parameterization for the global average forcing by stratospheric sulfuric acid aerosols assumes that for a small optical thickness ($\tau < 1$) the forcing is linear in τ and approximately 30 times the optical thickness (Lacis et al. 1992). This linearity holds true for instantaneous forcing at relatively small SZA also. Figure 2 shows the dependence of forcing on τ for four SZAs. Linearity holds for SZA $< \sim 55^\circ$. For larger SZAs, the relationship becomes an exponential of the form where

$$F(\tau) = a(1 - e^{-b\tau}) \quad (2)$$

a and b are constants. The relationship between forcing and relative humidity is also of a nonlinear nature for $RH > \sim 80\%$ (Nemesure et al. 1995) as a consequence of the hygroscopic growth of sulfate particles above the deliquescence point (Tang and Munkelwitz 1994). An expression relating forcing to RH is of the form

$$F(RH) = -a(1 - RH)^{-b} \quad (3)$$

where a and b are constants. Empirical relationships such as the ones in Equation (2) and Equation (3) can be used to more accurately calculate the forcing.

The marine distribution of Hoppel et al. (1990) (Figure 3) was chosen for the purpose of calculating the instantaneous direct forcing for October 15, 1986, at 18Z over the North Atlantic Ocean (Figure 4). The forcing was derived using sulfate column burden computed with a subhemispheric chemistry model driven by observation-derived meteorological data (Benkovitz et al. 1994). The contribution to the direct shortwave forcing in Figure 4 is evaluated as the clear sky forcing multiplied by the cloud free fractional area.

$$F_{\text{Direct}} = F_{\text{clear-sky}} (1 - cf) \quad (4)$$

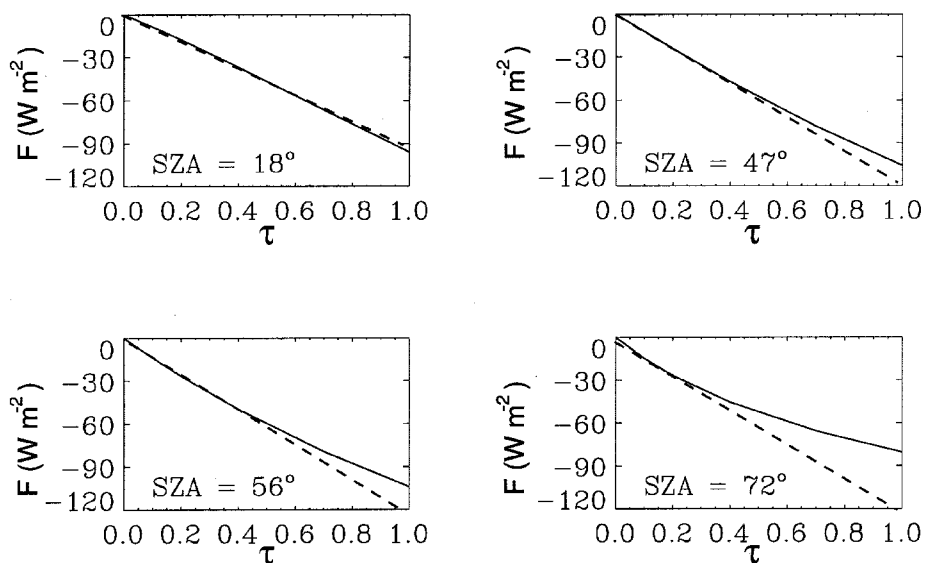


Figure 2. Direct forcing, ΔF versus optical thickness, τ (solid lines) for four solar zenith angles indicating the linearity (as shown by the dashed lines) between ΔF and τ . The calculations are for ammonium sulfate aerosol at $RH = 80\%$ and a dry particle radius, $r = 0.135 \mu\text{m}$.

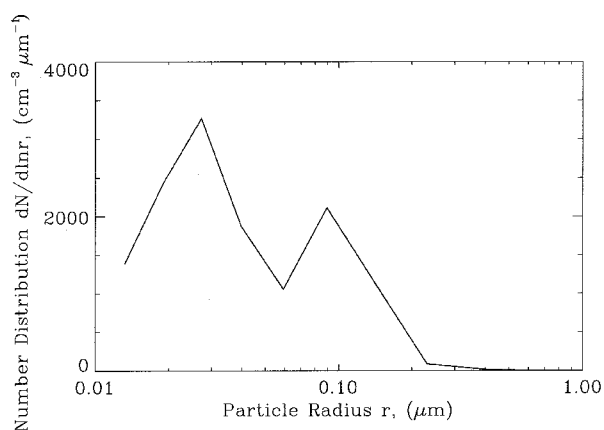


Figure 3. Marine aerosol number size distribution ($\text{cm}^{-3} \mu\text{m}^{-1}$) for the North Atlantic Ocean taken from differential mobility analyzer measurements in March 1983 (Hoppel et al. 1990).

where cf is the cloud fraction. Figure 4 shows peaks (-6 to -10 Wm^{-2}) in the direct forcing in the vicinity of the Gulf Stream off the North East coast of the United States as well as over the central North Atlantic. These (absolute) maxima in the forcing are collocated with high concentrations of sulfate computed by the chemistry model. The white areas in the figure represent regions where the direct effect is absent because these areas were entirely covered by clouds. The terminator line on the right side of the figure separates the regions where the sun is above the horizon to areas where sunset has already occurred.

Further investigation is necessary to address some considerations and limitations to this approach. For example, we used the RH in the boundary layer to define the hygroscopic growth of the aerosol in the entire column rather than a vertical profile of the RH. In addition, the vertical structure of the aerosol size distribution used to derive the forcing

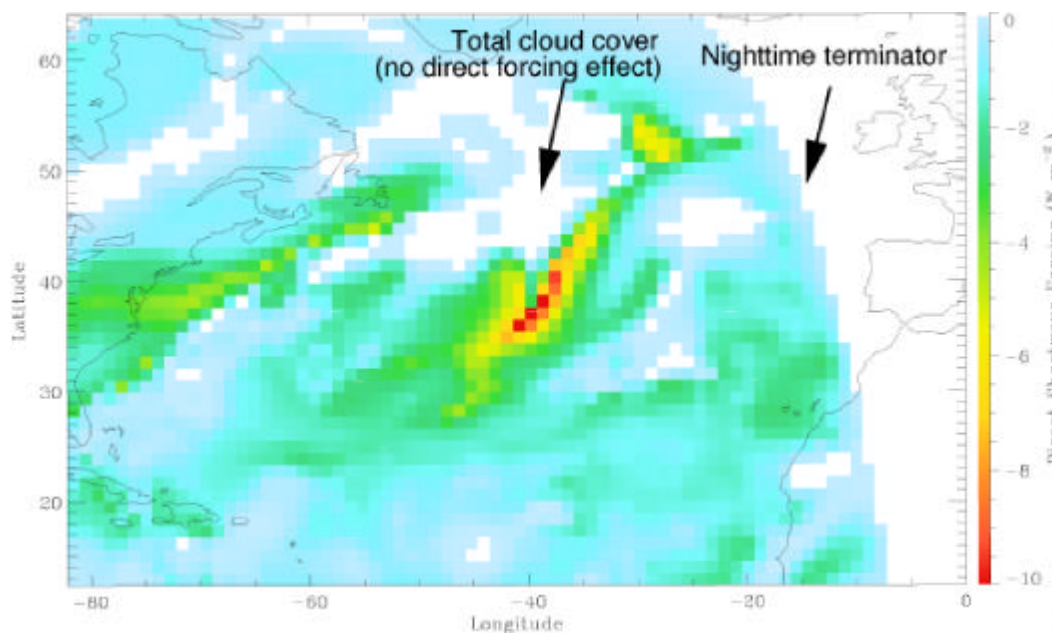


Figure 4. Direct shortwave forcing for October 15, 1986, at 18Z over the North Atlantic Ocean calculated using the summing method approach and the size distribution of Figure 3. Aerosol optical thickness data was obtained from sulfate column burden measurements from the chemistry model (Benkovitz et al. 1994); RH and cloud cover data were obtained from the European Centre for Medium Range Weather Forecasts (ECMWF) 6-hour forecast model output. Values indicated over land surfaces are approximate, because the effect of variable surface albedo has not been accounted for.

was limited to a single distribution for the entire column. Furthermore, the sensitivity of forcing to different aerosol size distributions and composition must be determined as well as the sensitivity to surface albedo. Once those issues have been addressed, it is believed that an approach can be developed that permits quick and accurate computation of the direct aerosol forcing in climate models based on modeled aerosol distributions.

A movie showing forcing as a function of time for several calendar months in 1986-87 has been prepared. For information e-mail seth@bnl.gov.

References

- Benkovitz, C. M., C. M. Berkowitz, R. C. Easter, S. Nemesure, R. Wagener, and S. E. Schwartz, 1994: Sulfate over the north Atlantic and adjacent continental regions: evaluation for October and November 1986 using a three-dimensional model driven by observation-derived meteorology, *J. Geophys. Res.*, **99**, 20725-20756.
- Coakley, J. A., R. D. Cess, and F. B. Yurevich, 1983: The effect of tropospheric aerosols on the earth's radiation budget: A parameterization for climate models, *J. Atmos. Sci.* **40**, 116-138.
- Hansen, J. and L. Travis, 1974: Light scattering in planetary atmospheres, *Space Sci. Rev.*, **16**, 527-610.
- Hoppel, W. A., J. W. Fitzgerald, G. M. Frick, and R. E. Larson, 1990: Aerosol size distributions and optical properties found in the marine boundary layer over the Atlantic Ocean, *J. Geophys. Res.*, **95**, 3659-3686.
- Lacis, A., J. E. Hansen, and M. Sato, 1992: Climate forcing by stratospheric aerosols, *Geophys. Res. Lett.*, **19(15)**, 1607-1610.
- Nemesure, S., R. Wagener, and S. E. Schwartz, 1995: Direct shortwave forcing of climate by anthropogenic sulfate aerosol: Sensitivity to particle size, composition, and relative humidity, *J. Geophys. Res.*, **100**, 26105-26116.
- Tang, I. N. and H. R. Munkelwitz, 1994: Water activities, densities, and refractive indices of aqueous sulfates and sodium nitrate droplets of atmospheric importance, *J. Geophys. Res.*, **99**, 18801-18808.